J. Anat. (1992) 180, pp. 89–95, with 6 figures Printed in Great Britain

Microvessel and astroglial cell densities in the mouse hippocampus

M. SHIMADA, N. AKAGI, H. GOTO, H. WATANABE, M. NAKANISHI, Y. HIROSE AND M. WATANABE

Department of Anatomy, Osaka Medical College, Japan

(*Accepted 14 August 1991*)

ABSTRACT

In order to study the factors responsible for glucose uptake in the mouse hippocampus, microvessel and astroglial cell densities were measured and compared in each laminal region. Microvessel density was examined on histologically prepared sections after injection of Indian ink and measured by means of an image analyser. Astroglial cell density was determined after the cells were stained immunohistochemically. Microvessel and astroglial cell densities were determined in 10 different hippocampal structures. Microvessel and astroglial cell densities were strongly correlated in all layers except the pyramidal cell layers. The highest density of perfused microvessels was found in the stratum lacunosum–moleculare, compared with other regions, and the lowest values were found in the stratum lucidum and dentate granular cell layer. Among pyramidal cell layers, microvessel density in sector CA3a was significantly higher than that in CA1.

INTRODUCTION

In recent years there has been growing interest in the relationship between energy metabolism and neuronal activity in the central nervous system. In a previous study we investigated differences in the uptake of radioactive 2-deoxyglucose and glucose in the mouse hippocampus (Shimada et al. 1989). We found that energy metabolism was most active in the stratum lacunosum-moleculare, and lowest in the dentate granular cell layers. Many investigators have suggested that capillary density or local blood circulation, enzyme activities, and pathway specificity are relevant to the uptake of glucose in the brain (Colin & Campbell, 1939; Ribak, 1981; Kageyama & Wong-Riley, 1982; Klein et al. 1986; Gross et al. 1987; Borowsky & Collins, 1989*a*, *b*). On the other hand, it is widely accepted that nerve cells are supplied with glucose from the blood circulation by glucose transport through the astrocytes which serve as a metabolic reservoir for neurons (Lund, 1979). To our knowledge, however, no study to date has investigated astroglial cell density as a factor for glucose uptake in the brain. In the present work, the densities of microvessel networks, which may reflect the blood circulation, and of astroglial cells reacting immunohistochemically with glial fibrillary acid protein (GFAP) were measured quantitatively in mouse hippocampal regions and compared with our previous data on glucose uptake (Shimada et al. 1989).

MATERIALS AND METHODS

Animals

Male albino mice of the ICR strain (Nihon Clea Co., Japan), weighing approximately 30 g, were studied. They were anaesthetised with sodium pentobarbital and perfused transcardially with 20–30 ml of 10 mM phosphate-buffered 0.9% (wt/vol) saline (PBS) at room temperature for 5 min, and then with 80–100 ml of 3.0% paraformaldehyde in 0.1 M phosphate buffer (pH 7.4) at room temperature for 30 min.

Measurement of microvessel density in the hippocampus

For the microvessel preparations, the mice were perfused with 20 ml of Indian ink diluted with 0.1 M phosphate buffer for 20 min. Indian ink perfusions were performed after perfusion with the fixative. The brains were then removed from the skull and

Correspondence to Professor M. Shimada, Department of Anatomy, Osaka Medical College, Takatsuki City, Osaka 569, Japan.

immersed in 10, 20, or 30% sucrose for 1 d at 4 °C. After freezing with dry ice-hexane, brains were cut into serial 50 μm thick coronal sections on a freezing microtome. The microtome was calibrated so that section thickness was accurate. In order to remove the sucrose, the sections were rinsed for several minutes in distilled water. Then they were mounted on gelatin-coated slides, dried on a hotplate, counterstained with 1% neutral red, and covered with a coverslip. In the hippocampus, microvessels, defined as blood vessels less than 10 μm in diameter, were assessed quantitatively using an image analyser (Luzex 3, Nikon, Japan). Microvessel density was expressed as percentage for a given area (in mm^2). In the Luzex 3 system, this percentage value was called the P-area of the single field. In the present work, P-area of the single field was expressed by the following formula:

$$\text{P-area of the single field} = \frac{\text{microvessel area in each layer}}{\text{total area of each layer}} \times 100.$$

For the measurement of the total area of individual layers, each layer on the colour monitor screen was precisely trimmed by the mouse-equipped pointer. The trimming was carried out at a magnification of 2.5×10. Because of the counterstaining with 1% neutral red, each region in the hippocampus was easily identified. In this system, the trimmed area, i.e. total area of each layer, was called the fractional area. Microvessels, black in colour, were easily differentiated from other tissues (Figs 2, 3). The measure modes for microvessel and fractional area in the image analyser were thus set up automatically. Each value for an individual mouse was determined from 5 serial sections.

Measurement of astroglial cell density in the hippocampus

For immunohistological study, animals were perfused further with 10% sucrose in the 0.1 M phosphate buffer at 4 °C (same volumes and rate as for the fixative) following perfusion with the fixative described above. Immediately after perfusion, brains were removed from the skulls, immersed in phosphate-buffered 30% sucrose for 2 d at 4 °C, and then frozen in a deep freezer at −80 °C until sectioning. Brains were cut into serial 40 μm coronal sections of by a cryotome at −30 °C. All sections were rinsed several times with 10 mM-PBS at 4 °C. Free-floating sections were immersed in 0.3% normal sheep serum dissolved in 2% PBS-Triton X overnight. The sections were then incubated for 2 d at 4 °C in rabbit serum against cow GFAP (Dakopatts, Denmark) diluted to 1:2000 with 2% PBS-Triton X. After rinsing several times with 2% PBS-Triton X at room temperature, sections were incubated for 3 h at room temperature in a biotinylated rabbit IgG diluted to 1:200 with 2% PBS-Triton X, and rinsed several times with 2% PBS-Triton X. Following the ordinary avidin–biotin complex method (Vecstain ABC Kit, Vector Lab., USA), tetramethyl benzidine was used for the peroxidase staining to yield a blue reaction product that shows superior sensitivity when compared with the brown reaction product in 3,3′-diaminobenzidine method (Mesulam, 1978). After several rinsings in distilled water, a series of sections was mounted on gelatin-coated slides, air-dried, and covered with a coverslip. GFAP-positive astroglial cells were observed as dark blue. The sections of various hippocampal regions were photographed and the cells counted in each given area. The density was expressed as cells/mm^2. Each value in the hippocampal regions for 1 mouse was from 5 serial sections.

Statistics

All statistical comparisons were made by a 2-tailed Student's t test. All values in each hippocampal region were reported as means from 4 animals. The correlation coefficient between capillary and astroglial cell densities was statistically evaluated with a single-factor analysis of variance.

RESULTS

Microvessel and GFAP-positive astroglial cell densities in each hippocampal region are shown in Tables 1 and 2. Vascularity in the hippocampus was rich, the microvessel density being significantly higher in the stratum lacunosum-moleculare than in the other hippocampal regions ($P < 0.02$), and lowest in the stratum lucidum and dentate granular layer ($P < 0.05$). As to the pyramidal cell layers, vascularity in the CA3a sector was significantly higher than that of other sectors ($P < 0.01$). In addition, the density of GFAP-positive astroglial cells in the stratum lacunosum-moleculare was also significantly higher than that of other hippocampal regions ($P < 0.01$), which may be consistent with the data for microvessel density. In contrast, the pyramidal cell and dentate granular layers had the lowest GFAP-positive cell density ($P < 0.01$). The hilum of the fascia dentata and the stratum lucidum also had significantly low cell density as compared with the strata oriens and moleculare ($P < 0.05$). The correlation coefficient (r) between microvessel and astroglial cell densities in the

Table 1. *Vascularity in the mouse hippocampus*

Hippocampal regions	Vascularity (% ± S.D.)	Significant at
Str. lacunosum-moleculare	30.5 ± 2.8	$P < 0.01$
Str. pyramidale (CA3a)	27.0 ± 3.9	
Str. moleculare	25.6 ± 2.3	$P < 0.01$
Str. pyramidale (CA3)	23.9 ± 1.6	$P < 0.05$
Hilus fascia dentata	22.0 ± 3.2	
Str. pyramidale (CA1)	20.6 ± 1.8	$P < 0.05$
Str. oriens	20.3 ± 2.1	$P < 0.05$
Str. radiatum	18.9 ± 2.4	
Str. lucidum	15.9 ± 2.0	$P < 0.05$
Str. granulosum	14.6 ± 3.2	

Table 2. *Cell density of GFAP-positive astroglia in the mouse hippocampus*

Hippocampal regions	Cell density (cells/mm² ± S.E.M.)
Str. lacunosum-moleculare	*2872 ± 77
Str. oriens	2256 ± 35
Str. moleculare	1804 ± 46
Str. radiatum	1538 ± 19
Str. lucidum	1450 ± 75
Hilus fascia dentata	1412 ± 30
Str. pyramidale (CA1, CA3)	180 ± 26
Str. granulosum	91 ± 8

* Significant at $P < 0.01$ as compared with other regions.

hippocampal regions, except for in the pyramidal cell layers, was 0.8207 (Fig. 1). This value was statistically significant at $P < 0.05$.

Morphological features of the microvessel network and the astrocyte in each hippocampal region are shown in Figures 2–6. In the stratum radiatum, microvessels arranged vertical to the pial surface were dominant (Fig. 3). while they showed a fine-mesh disposition in the stratum lacunosum-moleculare (Fig. 3). Astroglial cells in the strata pyramidale and granulosum were few in number (Fig. 4), while there were many in the stratum lacunosum-moleculare. Astroglial cells showed somewhat different profiles in each laminal region. In the strata oriens and radiatum and the dentate molecular layer, most of the glial cells appeared to have a long and slender perikaryon and many thick processes extending vertical to the pial surface (Fig. 5). Conversely, most of the cells in the stratum lacunosum-moleculare had a spherical perikaryon and many thin short processes extending in all directions, making a rather circular field with their somata (Fig. 6). In the dentate granular cell layer, astrocytes were few in numbers, but there were many fine fibres extending from the astrocytes in the subgranular zone (Fig. 4).

DISCUSSION

In order to clarify the factors responsible for glucose uptake in the hippocampus, we examined morphometric relationships between vascularity and density of astroglial cells that reacted immunohistochemically with GFAP. Three main conclusions can be drawn from the results. Firstly, the highest microvessel and astrocyte cell densities were seen in the stratum lacunosum-moleculare where glucose uptake was

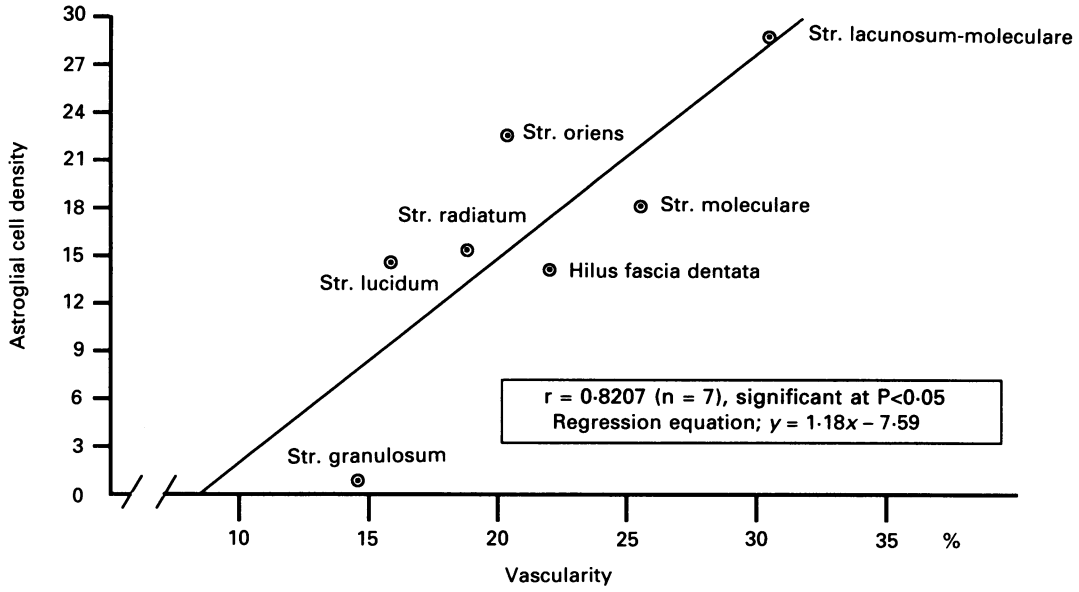

Fig. 1. Correlation between microvessel and astroglial cell densities.

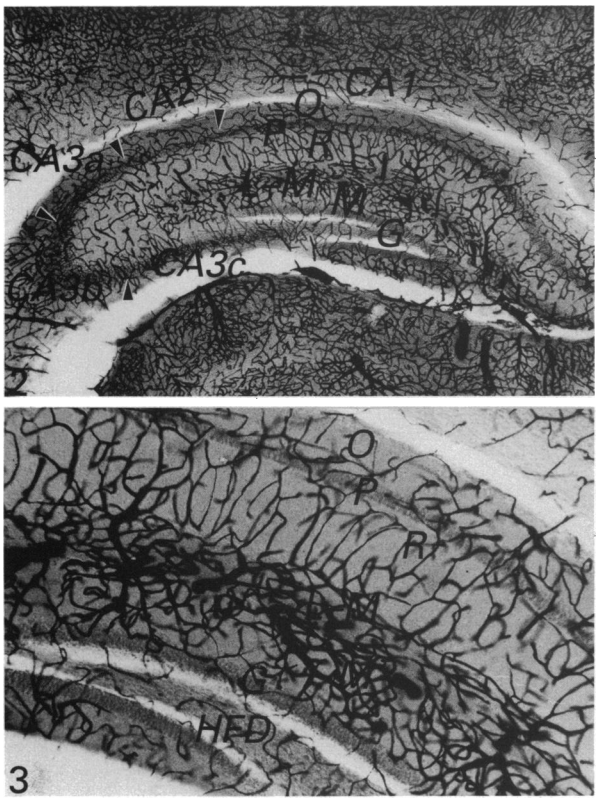

Fig. 2. Microvessel network in the hippocampus after injection of Indian ink and counterstaining with 1% neutral red. 2.5 × 4. Note high vascularity in the stratum lacunosum-moleculare (*L-M*) and pyramidal cell layer in CA3a. Arrows indicate the boundaries of each hippocampal sectors from CA1 to CA3. *O*, stratum oriens; *P*, stratum pyramidale; *R*, stratum radiatum; *L-M*, stratum lacunosum-moleculare; *M*, stratum moleculare; *G*, stratum granulosum.

Fig. 3. High-power microphotograph showing microvessel network in Ammon's horn. 2.5 × 10. Note the vertical microvessel arrangement in the stratum radiatum and fine-mesh network in the stratum lacunosum-moleculare. *O*, stratum oriens; *P*, stratum pyramidale; *R*, stratum radiatum; *L-M*, stratum lacunosum-moleculare; *M*, stratum moleculare; *G*, stratum granulosum; *HFD*, hilus fascia dentata.

most active. Secondly, microvessel and glial cell densities were low in the strata granulosum and pyramidale in CA1, where the glucose uptake was inactive. Thirdly, among hippocampal pyramidal cell layers, microvessel density was highest in the CA3a sector, where glucose uptake was most active. However, astroglial cell density in this sector was low, as in the CA1.

As to the factors responsible for glucose uptake in the brain, capillary density or local blood circulation, enzyme activity, and pathway specificity have all been advanced. Borowsky and Collins (1989*a*, *b*) suggested that the glucose utilisation may be partly associated with pathway specificity. They showed that the high glucose utilisation in the dentate molecular layer may be associated with the afferent connections. However, these perforant fibres from the lateral part of the entorhinal area may also distribute to the stratum lacunosum-moleculare (Raisman et al. 1965; Anderson et al. 1966; Hjorth-Simonsen & Jeune, 1972). Witter and Groenewegen (1984) showed precisely that the terminal field of the perforant path of the hippocampal region occupies the middle and outer part of the molecular layer of the dentate gyrus and the stratum lacunosum-moleculare of Ammon's horn. With regard to the projection of the entorhinal cortex to the hippocampal regions, the rostrolateral part of the entorhinal cortex does not contribute to the projection to the dentate gyrus, whereas it does give rise to fibres destined for CA1 and the subiculum. Successively more medial and caudal parts of the entorhinal cortex increasingly project to the dentate gyrus, whereas the projections to CA1 gradually diminish in density (Witter et al. 1988). Our earlier work showed the highest glucose uptake in the stratum lacunosum-moleculare. (Shimada et al. 1989). Therefore, if glucose uptake is dependent on afferents, then the perforant path from the rostrolateral parts of the entorhinal cortex might be more active in glucose metabolism than that from caudomedial parts.

On the basis of the data on blood–brain barrier (BBB) nutrient transport, it can be shown that by controlling nutrient availability in the brain, the BBB plays a significant and sometimes major role in the regulation of many pathways of brain metabolism (Partridge, 1983). Klein et al. (1986) found a close correspondence between local cerebral glucose utilisation measured autoradiographically and the density of perfused capillaries. The present data showed the highest vascularity in the stratum lacunosum-moleculare. These results partly support recent observations of a strong correlation between capillary density and glucose metabolism.

The stratum lacunosum-moleculare and the dentate molecular layer have the highest activities of the tricarboxylic acid (TCA) cycle enzymes, succinate dehydrogenase (Fried et al. 1966), malate dehydrogenase, and citrate synthetase (Wagman & Collins, 1988). Moreover, capillary density (Colin & Campbell, 1939) and glucose utilisation are maximal in these layers. Thus the large capacity for oxidative metabolism within these layers correlates with the density of microvessels and high rates of metabolic activity.

The highest levels of cytochrome oxidase, a marker enzyme for mitochondria, are found in the stratum lacunosum-moleculare of the hippocampus and the outer molecular layer of the dentate gyrus (Borowsky & Collins, 1989*a*, *b*; Ribak, 1981)). Electron micro-

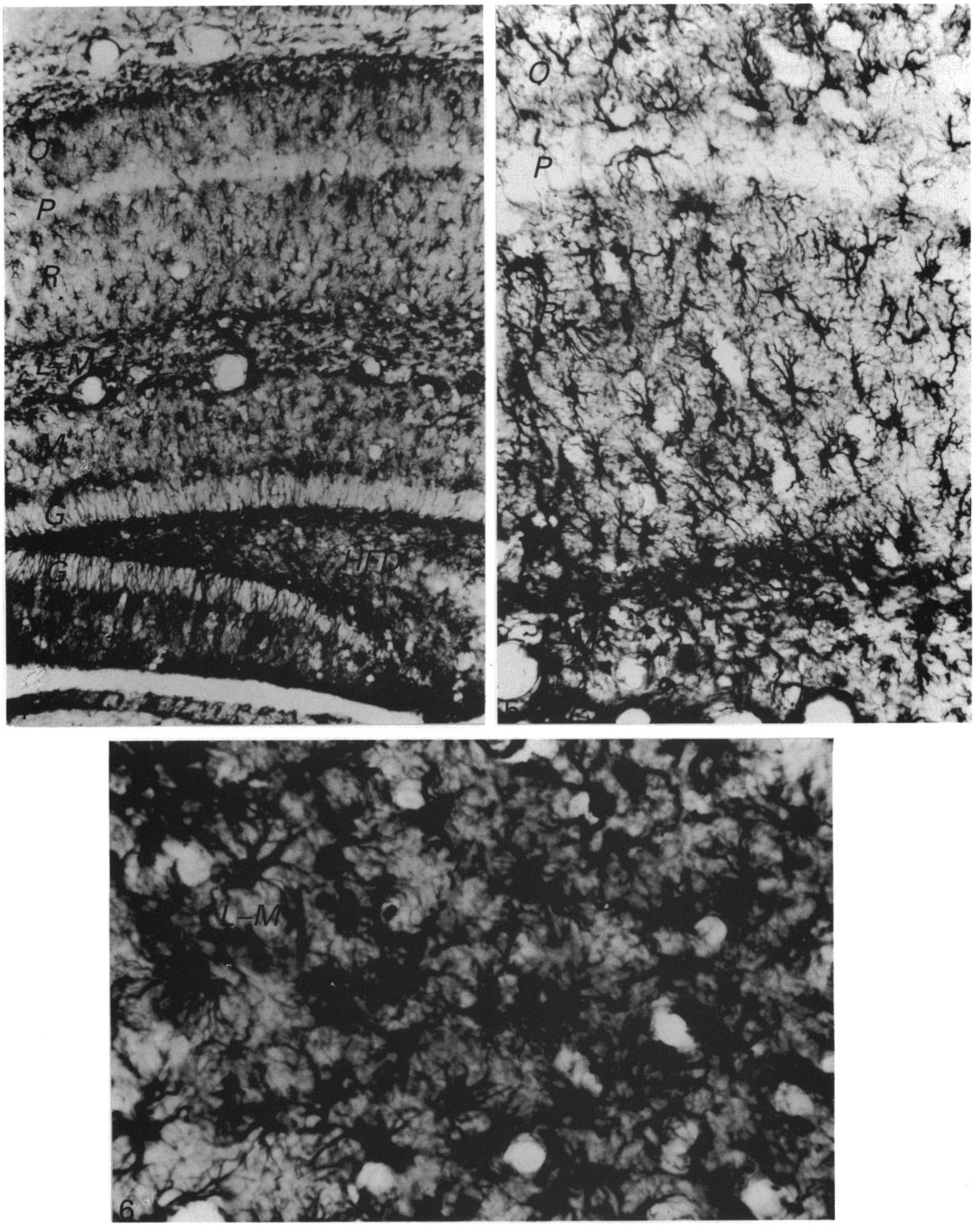

Fig. 4. Immunohistochemical localisation of GFAP in the hippocampus. 4 × 4. Note a few GFAP-positive astroglial cells in the stratum pyramidale and granulosum. *O*: Stratum oriens; *P*, stratum pyramidale; *R*, stratum radiatum; *L-M*, stratum lacunosum-moleculare; *M*, stratum moleculare; *G*, stratum granulosum; *HFD*, hilus fascia dentata.

Fig. 5. GFAP-positive astroglia in the stratum radiatum. 10 × 10. Most of the cells appear to have a long and slender perikaryon and many thick processes extending vertical to the pial surface. *O*, stratum oriens; *P*, stratum pyramidale; *R*, stratum radiatum; *L-M*, stratum lacunosum-moleculare.

Fig. 6. GFAP-positive astroglia in the stratum lacunosum-moleculare. 20 × 10. Note spherical perikaryon and short processes. *L-M*, stratum lacunosum-moleculare.

scopic analysis demonstrated that cytochrome oxidase activity was greatest in dendrites, and that axon terminals which formed synapses with the spines of these dendrites were much less reactive (Ribak, 1981; Kageyama & Wong-Riley, 1982). However, mitochondria are most intensely localised in the protoplasmic astroglia (Peters et al. 1976). Hence, high glucose uptake and astroglial cell density in this layer may be consistent with the highest activity of cytochrome oxidase. Although astroglial cells showed a different profile in each location, this may be related simply to the microvessel arrangement. Thus a spherical perikaryon and short processes of astroglia in the stratum lacunosum-moleculare might be encircled by the mesh-like capillary network, while the long and slender perikaryon and the perpendicular processes in the stratum radiatum, stratum oriens and dentate molecular layer seem to travel parallel with the microvessel. In addition, because of the very similar structural features of the astrocytes in the dentate molecular layer, astrocytes in Ammon's horn were supposed to be of the protoplasmic type (Kosaka & Hama, 1986; Eckenhoff & Rakic, 1987). We therefore speculate that these astrogial cells in Ammon's horn may be metabolically identical. Even if the cytochrome oxidase is equally distributed in the dentate molecular layer and the stratum lacunosum-moleculare, present and previous data (Shimada et al. 1989) showed that the glucose uptake and microvessel and astroglial cell densities were significantly high in the latter field. In addition, the present data showed that, as a whole, there was a close relationship between vascularity and astroglial cell density in all layers except for the pyramidal cell layer in CA3a ($r = 0.8207$, $P < 0.05$). We therefore speculate that, at least in the lacunosum-moleculare and dentate molecular layers, the factors responsible for glucose uptake might be astroglial cell density, because the astroglia may be closely related to the dendrites, and the capillary wall, rather than axon terminals (Cordero et al. 1982; Kosaka & Hama, 1986).

Kageyama and Wong-Riley (1982) showed that cytochrome oxidase staining in the somata of CA3 pyramidal cells and various interneurons was more intense than in CA1 pyramidal and dentate granule cells, while very low levels of cytochrome oxidase activity was observed in the stratum lucidum of CA3. The activity of cytochrome oxidase in CA3 and the stratum lucidum may be consistent with our previous data on glucose uptake, while high activity of cytochrome oxidase in the granular cell layer contradicts the finding of low glucose uptake in that layer. This means that glucose uptake may partly correspond to the levels of cytochrome oxidase activity.

It is of great interest that the pyramidal cell layer of CA3a showing high glucose uptake was significantly richer in vascularity than other pyramidal sectors, because the calcium-loaded neurons often forming confined groups are localised preferentially in the transition zone between the CA1 and the CA3 sectors, adjacent to CA3a (DeLeo et al. 1987). This means that the high glucose uptake in the pyramidal cell layer of CA3a may depend on neuronal activity rather than on astroglial cell density.

ACKNOWLEDGEMENTS

This work was supported by a Grant-in-Aid for Scientific Research (C-02670032) from the Ministry of Education, Science and Culture of Japan.

REFERENCES

ANDERSON P, HOLMQVIST B, VOORHOEVE PE (1966) Excitatory synapses on hippocampal apical dendrites activated by entorhinal stimulation. *Acta Physiologica Scandinavica* **66**, 461–472.

BOROWSKY IW, COLLINS RC (1989*a*) Metabolic anatomy of brain: a comparison of regional capillary density, glucose metabolism, and enzyme activities. *Journal of Comparative Neurology* **288**, 401–413.

BOROWSKY IW, COLLINS RC (1989*b*) Histochemical changes in enzymes of energy metabolism in the dentate gyrus accompany deafferentation and synaptic reorganization. *Neuroscience* **33**, 253–262.

COLIN A, CAMPBELL P (1939) Variation in vascularity and oxidase content in different regions of the brain of the cat. *Archives of Neurology and Psychiatry* **41**, 223–242.

CORDERO ME, ZVAIGHAFT A, MUZZO S, BRUNSER O (1982) Histological maturation of astroglial cells in the archicortex of early malnourished rats. *Pediatric Research* **16**, 187–191.

DELEO J, TOTH L, SCHUBERT P, RUDOLPHI K, KREUTZBERG GW (1987) Ischemia-induced neuronal cell death, calcium accumulation, and glial response in the hippocampus of the Mongolian gerbil and protection by propentofylline (HWA 285). *Journal of Cerebral Blood Flow and Metabolism* **7**, 745–751.

ECKENHOFF MF, RAKIC P (1984) Radial organization of hippocampal dentate gyrus: a Golgi, ultrastructural, and immunocytochemical analysis in the developing rhesus monkey. *Journal of Comparative Neurology* **223**, 1–21.

FRIEDE RL, FLEMING LM, KNOLLER M (1966) A comparative mapping of enzymes involved in hexose monophosphate shunt and citric acid cycle in the brain. *Journal of Neurochemistry* **10**, 263–277.

GROSS PM, NADINE MS, PETTERSEN SE, PANTON DG, FENSTERMACHER JD (1987) Topography of capillary density, glucose metabolism, and microvascular function within the rat inferior colliculus. *Journal of Cerebral Blood Flow and Metabolism* **7**, 154–160.

HJORTH-SIMONSEN A, JEUNE B (1972) Origin and termination of the hippocampal perforant path in the rat studied by silver impregnation. *Journal of Comparative Neurology* **144**, 215–232.

KAGEYAMA GH, WONG-RILEY MTT (1982) Histochemical localization of cytochrome oxidase in the hippocampus: correlation with specific neuronal types and afferent pathways. *Neuroscience* **7**, 2337–2361.

KLEIN B, KUSCHINSKY W, SCHRÖCK H, VETTERLEIN F (1986) Independency of local capillary density, blood flow, and metabolism in rat brains. *American Journal of Physiology* **251** (*Heart Circulation Physiology* **20**), H1333–H1340.

KOSAKA T, HAMA K (1986) Three-dimensional structure of astrocytes in the rat dentate gyrus. *Journal of Comparative Neurology* **249**, 242–260.

MESULAM M-M (1978) Tetramethyl benzidine for horseradish peroxidase neurochemistry: a non-carcinogenic blue reaction-product with superior sensitivity for visualizing neural afferents and efferents. *Journal of Histochemistry and Cytochemistry* **26**, 106–117.

LUND AH (1979) Transport of glucose from blood to brain. *Physiological Reviews* **59**, 305–352.

PARTRIDGE WM (1983) Brain metabolism: perspective from the blood-brain barrier. *Physiological Reviews* **63**, 1481–1535.

PETERS A, PALAY SL, WEBSTER H DEF (1976) *The Structure of the Nervous System: The Neurons and Supporting Cells*, pp. 233–248. Philadelphia: W.B. Saunders.

RAISMAN G, COWAN WM, POWELL TPS (1965) The extrinsic afferent, commissural and association fibres of the hippocampus. *Brain* **88**, 963–996.

RIBAK CE (1981) The histochemical localization of cytochrome oxidase in the dentate gyrus of the rat hippocampus. *Brain Research* **212**, 169–174.

SHIMADA M, SHIMONO R, OZAKI HS (1989) Freeze-mount micro-autoradiographic study in the mouse hippocampus after intravenous injection of tritiated 2-deoxyglucose and glucose. *Neuroscience* **31**, 347–354.

WAGMAN IL, COLLINS RC (1988) Red and white metabolism in hippocampus. *Neurology* **38** (Suppl. 1), 181.

WITTER MP, GROENEWEGEN HJ (1984) Laminal origin and septotemporal distribution of entorhinal and perirhinal projections to the hippocampus in the cat. *Journal of Comparative Neurology* **224**, 371–385.

WITTER MP, GRIFFIOEN AW, JORRISTMA-BYHAM B, KRIJINEN JLM (1988) Entorhinal projections to the hippocampal CA1 region in the rat: an underestimated pathway. *Neuroscience Letters* **85**, 193–198.